Nanoscale Advances

ROYAL SOCIETY OF CHEMISTRY

PAPER

View Article Online
View Journal | View Issue

Cite this: *Nanoscale Adv.*, 2025, **7**, 5093

Nucleobase self-assembly: aggregation, morphological characterization, and toxicity analysis†

Raj Dave,‡[a] Ankita Jaiswal,‡[b] Ankur Singh,[c] Anam Naseer,[d] Monisha Patel,[a] Aamir Nazir,*[de] Dhiraj Bhatia,*[c] Nidhi Gour*[a] and Sandeep Verma*[b]

This study expands the platform for amyloidogenic building blocks, such as nucleobases, and their self-assembly. Here, we examine the self-assembly profile of nucleobases such as guanine, cytosine, and thymine and determine that these nucleobases, while aged, produce small globules which gradually transform into fibrillar assemblies. Notably, the amyloid-like fibrillation in adenine and uracil has already been reported; hence, it was imperative to understand the amyloidogenic propensity in these unexplored nucleobases. The aggregates formed by guanine, cytosine, and thymine interestingly reveal a distinctive spectrum characteristic of amyloidogenic proteins after binding to the amyloid-specific dye Thioflavin T (ThT). The MTT assay in human retinal pigment epithelial RPE-1 cell lines revealed the aggregates formed by these nucleobases are toxic with significantly more toxicity observed for aged samples as compared to the fresh ones. The *in vivo* assays in *C. elegans* nematodes further validated the toxicities induced by the aggregates and the heat shock survival assay suggests these metabolite assemblies affect the protein clearance machinery like other amyloids. Overall, the research offers additional support for the role of amyloidogenesis in IEMs and suggests a recognized toxicity mechanism for IEMs caused by the accumulation of nucleobases.

Received 19th March 2025
Accepted 23rd June 2025

DOI: 10.1039/d5na00259a

rsc.li/nanoscale-advances

Introduction

The development of highly complex systems relying on supramolecular interactions is essential for constructing self-assembled structures that mimic biological traits. Nucleobase interactions play a pivotal role in transcription and translation, among other biological activities in living organisms. Their versatile frameworks and adaptive material properties, including stimulus responsiveness, extracellular interactions, and structural self-repair, have garnered significant interest. Numerous hierarchical self-assembled systems mediated by nucleobase interactions have been engineered, aiming to advance applications in neurological and genetic disorders by leveraging their unique properties.[1] DNA base pairing is driven by nucleobase interactions, which serve as the blueprint of life due to their exceptional fidelity, molecular recognition capabilities, sequence specificity, and directional nature. These interactions are fundamental to the chemistry of nucleic acids, as the complementary hydrogen bonding between adenine (A) and thymine (T), and between guanine (G) and cytosine (C), stabilizes the DNA double helix structure.[2] Nucleobase interactions have been extensively studied due to their fundamental role in molecular recognition, self-assembly, and genetic information storage. The synthesis of highly ordered biomimetic materials through controlled assembly of bioinspired molecular building blocks has been a fast-expanding field of study in the disciplines of functional materials, biomedicine, and bioengineering processes. Diseases such as Alzheimer's, Parkinson's, and inborn errors of metabolism (IEMs) are associated with the formation and accumulation of highly ordered amyloid fibrillar structures derived from various metabolites.[3] Furthermore, it was suggested that phenylalanine's apparent ability to produce amyloid-like fibrils might provide new mechanistic understanding of the pathophysiology of phenylketonuria (PKU), the most common IEM illness caused by a malfunction in phenylalanine metabolism. Furthermore, the synthesis of hazardous metabolite fibrillar assemblies may also have an impact on the pathogenesis of retinal oxalosis.[4] Metabolites that are toxic or interfere with the normal function of cells and tissues accumulate and cause problems in most

[a]*Department of Chemistry, Indrashil University, Kadi, Mehsana, Gujarat, India. E-mail: gournidhi@gmail.com; nidhi.gour@indrashiluniversity.edu.in*

[b]*Department of Chemistry, Indian Institute of Technology Kanpur, India. E-mail: sverma@iitk.ac.in*

[c]*Department of Biomedical Engineering, Indian Institute of Technology Gandhinagar, India. E-mail: dhiraj.bhatia@iitgn.ac.in*

[d]*Academy of Scientific and Innovative Research (AcSIR), Ghaziabad 201002, India*

[e]*Division of Toxicology & Experimental Medicine, CSIR-Central Drug Research Institute, Lucknow, 226031, India. E-mail: anazir@cdri.res.in*

† Electronic supplementary information (ESI) available. See DOI: https://doi.org/10.1039/d5na00259a

‡ These authors contributed equally.

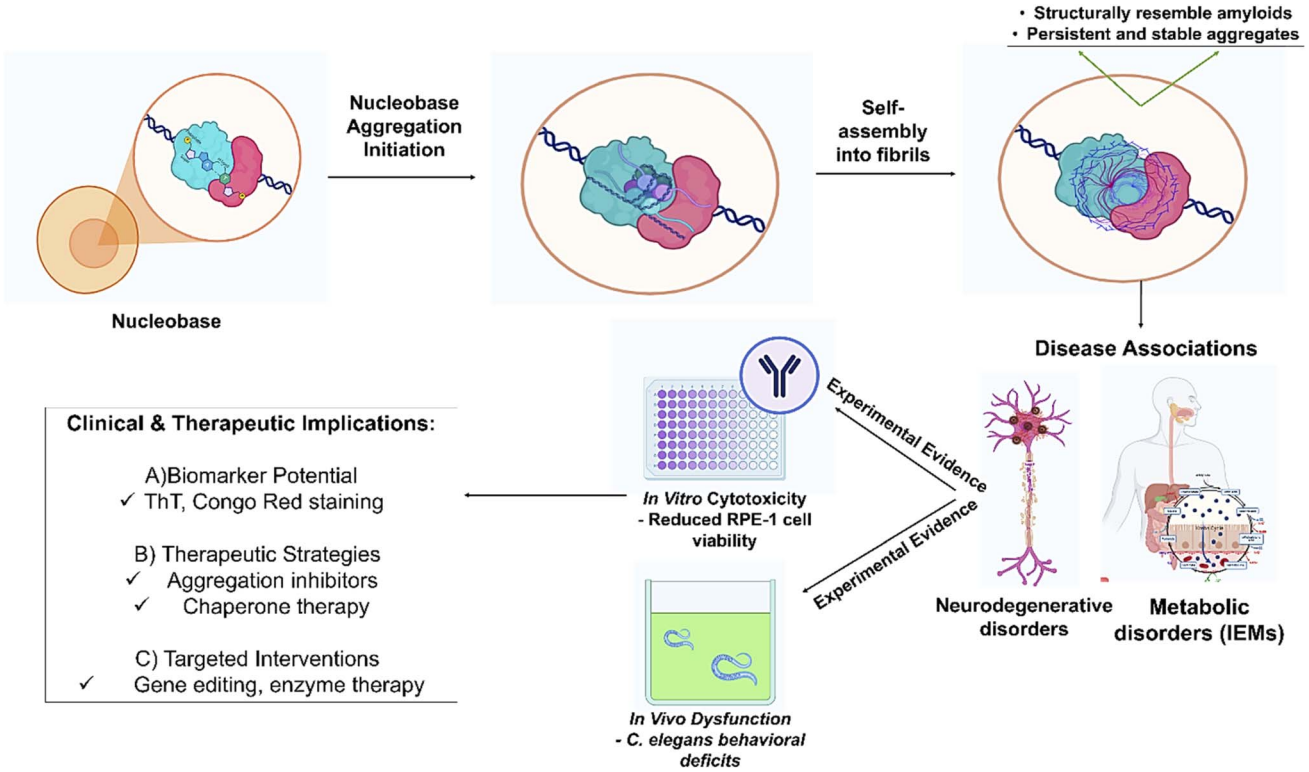

Fig. 1 Schematic representation of nucleobase interactions, detection methods, and biological implications. The figure illustrates nucleobase aggregation, experimental analysis techniques, and their physiological significance.

IEM disorders. Over fifty metabolic illnesses have been described and reported thus far. Metabolic disorders account for a significant portion of paediatric genetic diseases, but less than 1 in 250 000 people in most communities are affected by most of these issues.[5] Even though amyloid is believed to be associated with disease, functional amyloids and amyloid-like materials composed of proteins have been discovered to function in a wide range of biological systems, including catalytic functions in mammalian melanosomes and structural roles in bacterial biofilms and hyphae.[6] Here, we present an in-depth analysis of advancements in the biological approach concerning the physicochemical properties of functional nucleobases and their assembly. An overview diagram explaining the series of events leading to DNA nucleobase mutations, which ultimately cause autoimmune diseases, is shown in Fig. 1.

Results and discussion

Amyloid-like structure formation by nucleobases such as adenine and uracil has been previously reported. The self-assembly of adenine has been deciphered *in vivo* in a yeast model, and the toxicity associated with its intracellular accumulation suggests the role of amyloidosis in IEM caused by an excess of adenine, namely APRT syndrome.[7] Both adenine and uracil assemble into cytotoxic fibres; hence, motivated by these studies, we were compelled to thoroughly examine the self-assembling characteristics of guanine, cytosine, and thymine to investigate whether these nucleobases also possess the ability to self-assemble and form amyloid-like structures.[8] Therefore, by dissolving nucleobases in deionized (DI) water at various concentrations of 10 mM, 1 mM, and 100 μM, their ability to self-assemble was examined. As a control, we also studied the self-assembly of adenine and uracil along with these nucleobases. Optical microscopy was used to study the self-assembled structures, and the results show that both adenine and uracil form thin fibrillar assemblies that resemble amyloid-like structures, as reported previously. Initially, in fresh samples, small dispersed fibrils were observed, which over time underwent elongation and increased bundling, forming denser, more interconnected networks. By day 5, the fibrillar structures displayed higher entanglement and clustering, indicative of a maturation process in their self-assembly (Fig. S-1 and S-4†). These observations align with the progressive nature of amyloid-like fibrillation, where protofibrils nucleate, elongate, and later develop into more stable aggregates over time.[9,10] Given that adenine and uracil have previously been shown to exhibit amyloid-like aggregation, we were inspired to thoroughly investigate the aggregation and self-assembly properties of unexplored cytosine and guanine using microscopy and spectroscopy techniques. Cytosine's chemical structure is shown in Fig. 2a. We resorted to field emission scanning electron microscopy (FESEM) to achieve better resolution. The FESEM images of cytosine showed random aggregates (Fig. 2b) in fresh condition, while after 10 days of ageing, they changed to dense fibrillar structures (Fig. 2c, d, S-5 and S-6†). To learn more about the ultra-structure of the fibers and evaluate their

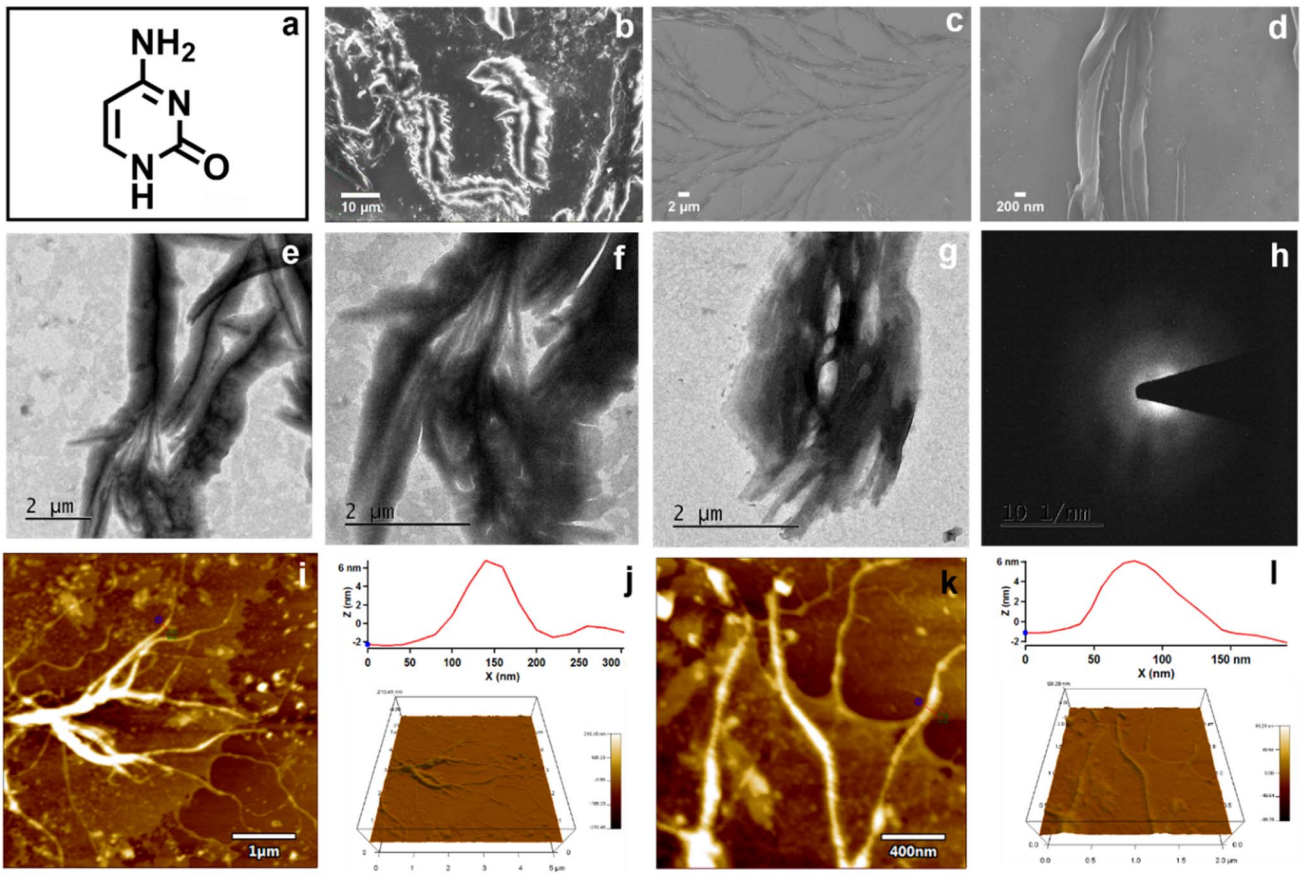

Fig. 2 Self-assembly of cytosine (100 μM). (a) Chemical structure of cytosine; (b) SEM of cytosine in fresh condition (Day-1); (c and d) SEM of cytosine after ageing (Day-10); (e–g) TEM of Cytosine after ageing (Day-10); (h) SAED pattern of cytosine suggesting the amorphous nature of aggregates; (i and k) 2D AFM micrograph of cytosine after ageing (Day-10); (j and l) 3D AFM micrograph of cytosine after ageing. (Day-10).

molecular packing, Transmission Electron Microscopy (TEM) was used to examine the aged cytosine samples. The thin fibrillar gel-like structures found in the TEM examinations of the aged cytosine are also visible (Fig. 2e–g). The Selected Area Electron Diffraction (SAED) pattern was examined with TEM micrographs. It should be emphasized that every point in the SAED pattern indicates a valid diffraction condition. Polycrystalline materials have a ring pattern, whereas single-crystalline materials have a stunning dotted ring pattern or a spot pattern. A thick, diffused ring characterizes amorphous materials.[11] The SAED pattern (Fig. 2h) suggests that these structures might be soft and amorphous in nature. Additionally, atomic force microscopy (AFM) revealed fibrillar aggregates formed by aged cytosine as shown in Fig. 2i and k. Fig. 2l shows that the height and diameter of the cytosine fibers are approximately 6 nm and 120 nm. Furthermore, fresh cytosine displayed a thick fibre-like bundle at 100 μM. This was comparable to what was observed using an optical microscope (OM). While fibril formation was observed in the early stages of nucleobase self-assembly, some images post-day 5 (Fig. S5 and S6†) suggest a reduction in visible fibrillar structures. This observation may be attributed to structural maturation, where fibrils transition into denser aggregates that are less distinguishable under conventional imaging conditions. Additionally, dynamic self-assembly processes, including disaggregation or further molecular rearrangement, could contribute to variations in fibril visibility over time. Future investigations using real-time spectroscopic and high-resolution imaging techniques will further elucidate the stability and long-term behavior of these nucleobase aggregates.

Additionally, thymine self-assembling studies were conducted similarly. Fig. 3a depicts the chemical structure of thymine. Tiny globular morphologies may be seen in the FE-SEM images of fresh Thymine (Fig. 3b, S-7 and S-8†). However, after ageing, they transformed into flake-like fibrous structures with different sizes and morphology (Fig. 3c, d, S-7 and S-8†). Both extremely thin and dense fibrillar bundles were seen in the TEM (Fig. 3e–g). The soft, amorphous nature of the fibers can be inferred from the SAED pattern (Fig. 3h). Moreover, the TEM observation was also supported by AFM micrographs (Fig. 3i–l) which revealed thick fibril bundle-like morphologies. Fig. 3l shows that the height and diameter of the thymine fibers are 40 nm and 600 nm.

Further, the self-assembly properties of guanine were also examined in detail. Interestingly, some hydrophilic properties were suggested by the chemical structure of guanine (Fig. 4a) as compared to cytosine and thymine. Initially, the self-assembled structures formed by guanine were examined using an optical

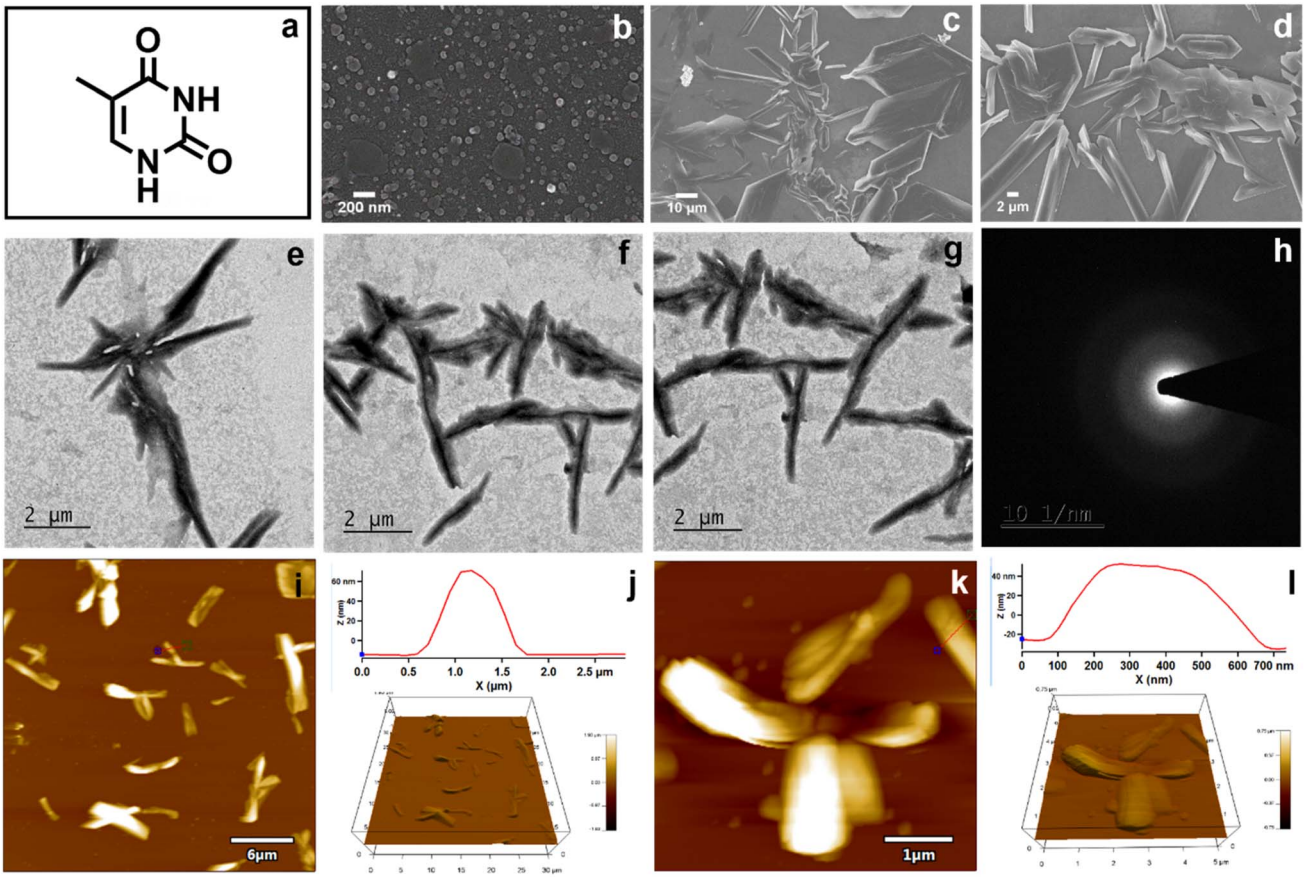

Fig. 3 Self-assembly of thymine (1 mM). (a) Chemical structure of thymine. (b) SEM of thymine in fresh condition (Day-1); (c and d) SEM of thymine after ageing (Day-10); (e–g) TEM of thymine after ageing (Day-10); (h) SAED pattern of thymine suggesting the amorphous nature of aggregates; (i and k) 2D AFM micrographs of thymine after ageing (Day-10); (j and l) 3D AFM micrographs of thymine after ageing (Day-10).

microscope followed by FESEM analysis, which revealed the presence of tiny globular aggregates all throughout in the fresh condition (Fig. 4b, S-9 and S-10†). As this solution matured, the globules tended to come together and formed clustered aggregates (Fig. 4c, d, S-9 and S-10†). The observations made upon ageing were also confirmed by the TEM images, which showed fused globular aggregates at different resolutions (Fig. 4e–g). The soft character of Guanine assemblies may be ascertained by the SAED pattern (Fig. 4 h). The AFM micrograph supported the SEM and TEM observations as well. Globular aggregates were also visible in the 2D AFM micrographs (Fig. 4i and k). The uneven topology of the globules in 3D AFM suggests that their surface is not smooth, which may be related to the aggregated globules seen in the SEM (Fig. 4j and l). Fig. 4l shows that the height and diameter of the guanine aggregates are 30 nm and 480 nm.

Notably, when the solution containing these nucleobases was heated to a high temperature and then gradually cooled, an enhanced aggregation that resembled an aged solution was also seen. (Fig. S-11†). This suggests molecules tend to aggregate with time or under external stimuli like temperature, which will induce enhanced intermolecular forces. Thioflavin T (ThT) experiments were carried out to determine the amyloid character of the aged aggregates of cytosine, thymine, and guanine.[12] It is well known that ThT binds to hydrophobic pockets of amyloidogenic structures which increases its fluorescence.[13] In Fig. 5a, the increase in fluorescence intensity suggests nucleobase-specific aggregation behavior over time in the presence of ThT. Interestingly, ThT fluorescence was enhanced when cytosine, thymine, and guanine were present. Additionally, microscope staining investigations demonstrated the effective binding of aggregates of cytosine, thymine, and guanine with ThT and Congo red as the structures revealed green fluorescence and apple green birefringence. Surprisingly, morphological changes were also visible as the aggregates tended to become more fibrillar with the addition of ThT and Congo red (Fig. 5b–d and S-12–S-16†).[14] The fluorescence increase is attributed to the formation of amyloid-like aggregates rather than prolonged dye incubation. While our results support aggregation as the main driver of fluorescence enhancement, we acknowledge that prolonged dye exposure or non-specific interactions may also contribute to it. Our future endeavours will aim to study the interaction of aggregates with ThT and CR in more detail *via* biophysical assays as well as MD simulation to understand their binding mechanism.

In order to understand the function of solubility factors and the balance between hydrophobic and hydrophilic groups in aggregation, we also investigated the impact of solvents on the

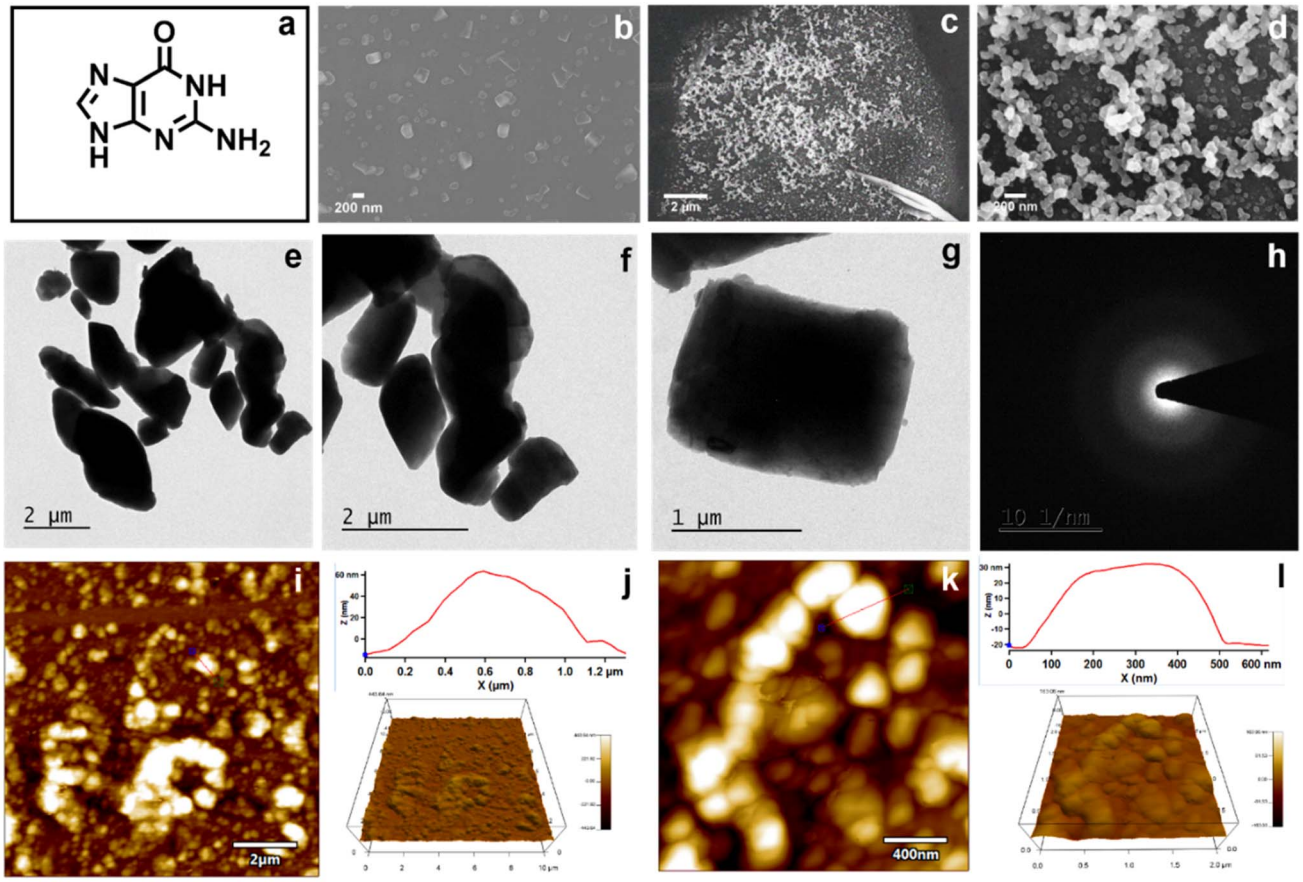

Fig. 4 Self-assembly of guanine (1 mM). (a) Chemical structure of guanine; (b) SEM of guanine in fresh condition under different magnification (Day-1); (c and d) SEM of guanine after ageing (Day-10); (e–g) TEM of guanine after ageing (Day-10); (h) SAED pattern of guanine suggesting the amorphous nature of aggregates; (i and k) 2D AFM micrographs of guanine after ageing (Day-10); (j and l) 3D AFM micrographs of guanine after ageing (Day-10).

self-assembly of adenine, uracil, cytosine, thymine and guanine. As a result, we looked at how cytosine self-assembles in different THF: water and methanol: water ratios. Because THF is an aprotic and somewhat non-polar solvent it may solubilize the aggregates (Fig. S-17–S-21†). Additionally, we investigated the relationship between methanol and water to comprehend how the development of structures changes as methanol concentration increases (Fig. S-22–S-26†). Comparing the methanol: water system to the THF: water system, it is clear from these results that the cytosine fibers are not as damaged. One possible explanation for the altered solubility parameters could be THF is an apolar protic solvent. Comparing the methanol:water system to the THF:water system, it is evident that cytosine fibers exhibit greater stability in methanol:water, whereas in THF:water, significant disruption of the assemblies is observed. This can be attributed to differences in solubility parameters, as THF is a polar aprotic solvent, which may alter hydrogen bonding interactions and disrupt fiber formation. The observed effects are not limited to cytosine; similar trends were noted for thymine and guanine, where THF:water systems led to partial disassembly of aggregates, whereas methanol:-water maintained fibrillar integrity to a greater extent. The results suggest that solvent polarity and hydrogen bonding capacity play crucial roles in driving nucleobase self-assembly, with aprotic solvents promoting aggregate disruption, while protic solvents stabilize hydrogen-bonded networks. (Fig. S-17–S-21 and S-27–S-31†). Moreover, to understand the effect of hydrogen bonding interactions in detail the FTIR spectra of cytosine, thymine and guanine were recorded before and after self-assembly. Notably, after 10 days, the spectra exhibited broadening in the N–H stretching region (~3200–3400 cm^{-1}) and the C=O stretching region (~1650–1700 cm^{-1}), indicative of enhanced intermolecular hydrogen bonding. This broadening, rather than mere intensity reduction, suggests the formation of a more extensive hydrogen-bonding network as the nucleobases undergo self-assembly over time (Fig. S-32–S-34†).

Furthermore, to gain a better understanding of the mechanism of self-assembly and its effects on cross-seeding, urea and tannic acid (TA) were co-incubated with adenine (A), thymine (T), uracil (U), guanine (G), and cytosine (C). Urea is one of the well-known hydrogen bond breakers. In light of this, if urea and the nucleobase assemblies are co-incubated, it is feasible to deduce the involvement of hydrogen bonding interaction. An equivalent generic amyloid inhibitor is called tannic acid (TA).[15] All amyloid-like structures are inhibited by TA. Interestingly, adding urea to this nucleobase solution caused the fibrous

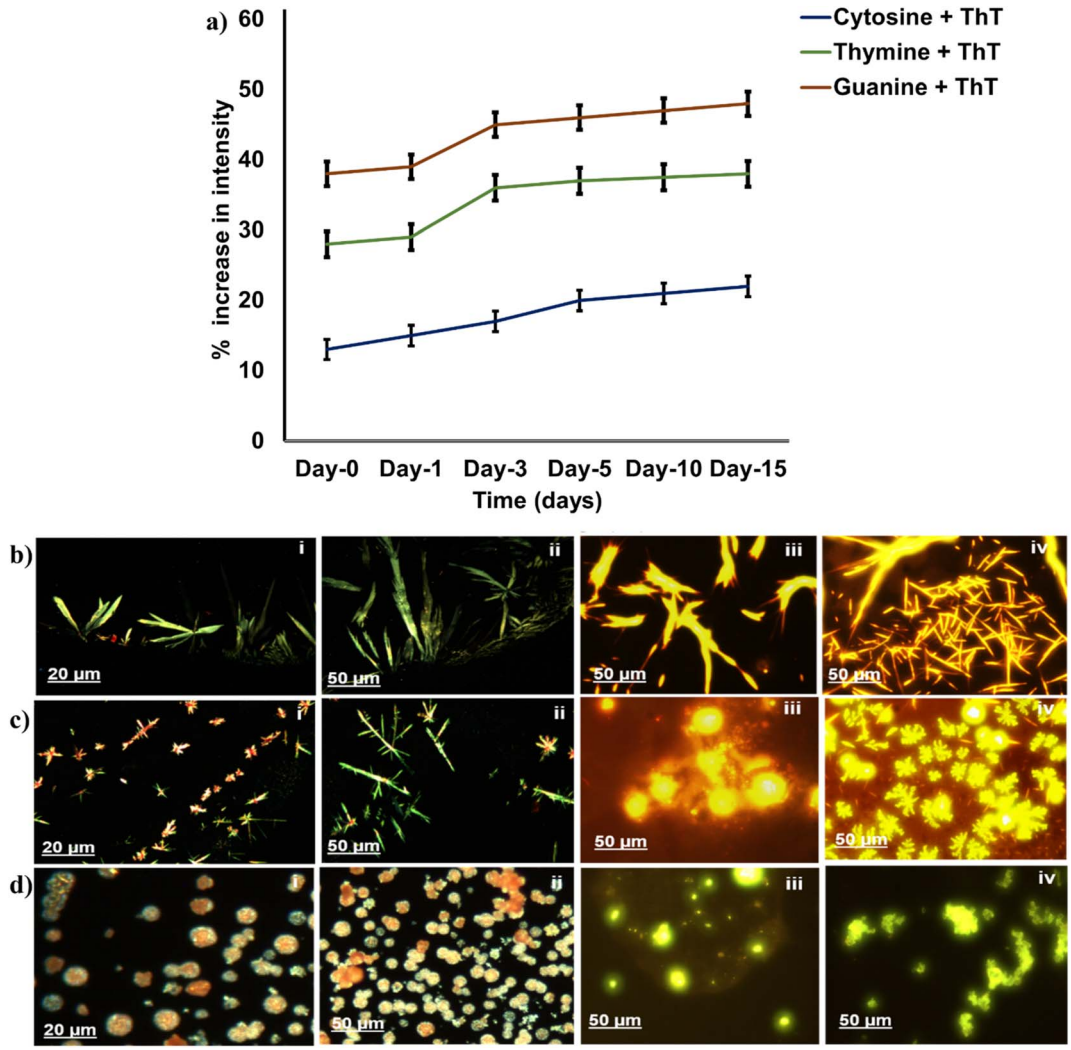

Fig. 5 (a) Percentage increase in fluorescence intensity of cytosine + ThT, thymine + ThT, and guanine + ThT measured over 15 days; (b) microscopy images of ThT and CR-stained bound with cytosine in (i) fresh condition in CR-stained; (iii) fresh condition in the green filter; (ii) on day 5 in CR-stained; (iv) day 5 in the green filter; (c) microscopy images of ThT and CR-stained bound with thymine in (i) fresh condition in CR-stained; (iii) fresh condition in the green filter; (ii) on day 5 in CR-stained; and (iv) day 5 in the green filter; (d) microscopy images of ThT and CR-stained bound with guanine in (i) fresh condition in CR-stained; (iii) fresh condition in the green filter; (ii) on day 5 in CR-stained; and (iv) day 5 in the green filter.

morphology to alter to globular sphere-like forms as shown in Fig. S-36.† According to the observation, hydrogen bonding interactions appear to be important, and in the absence of hydrogen bonding, π–π stacking interactions would take place.[16] However, when hydrogen bonding is present, the globules tend to fuse to form thick bundles that resemble fibril morphology. In addition, the morphologies changed to small globules in the presence of TA as mentioned in Fig. S-36.† However, the tendency to aggregate was much lower than it was when urea was present. This finding reaffirmed that π–π stacking is the primary interaction, even if aggregation may still happen if hydrogen bonding is the only driving force. In adenine (A), thymine (T), uracil (U), guanine (G), and cytosine (C), π–πstacking and hydrogen bonding combine to form a clustered fibril bundle. When these interactions operate independently, though, little globular aggregates will become apparent.[17]

The MTT assay is a fast colorimetric test that counts the number of live cells by detecting the cleavage of the tetrazolium ring of MTT (3-(4,5-dimethylthazol-2-yl)-2,5-diphenyl tetrazolium bromide) by dehydrogenases in active mitochondria. Many amyloids are toxic because they damage cell membranes; hence, we were driven to examine the influence of these nucleobase aggregates on cell survival. To test these ideas, we used MTT assays on human pigment epithelial RPE-1 cell lines by treating them with fresh and aged cytosine, thymine and guanine assemblies (Fig. 6).

To substantiate the results obtained from *in vitro* analyses, we opted for *in vivo* studies. For this, we employed *Caenorhabditis elegans* as our model organism. We studied the behavioral as well as physiological aspects after employing the

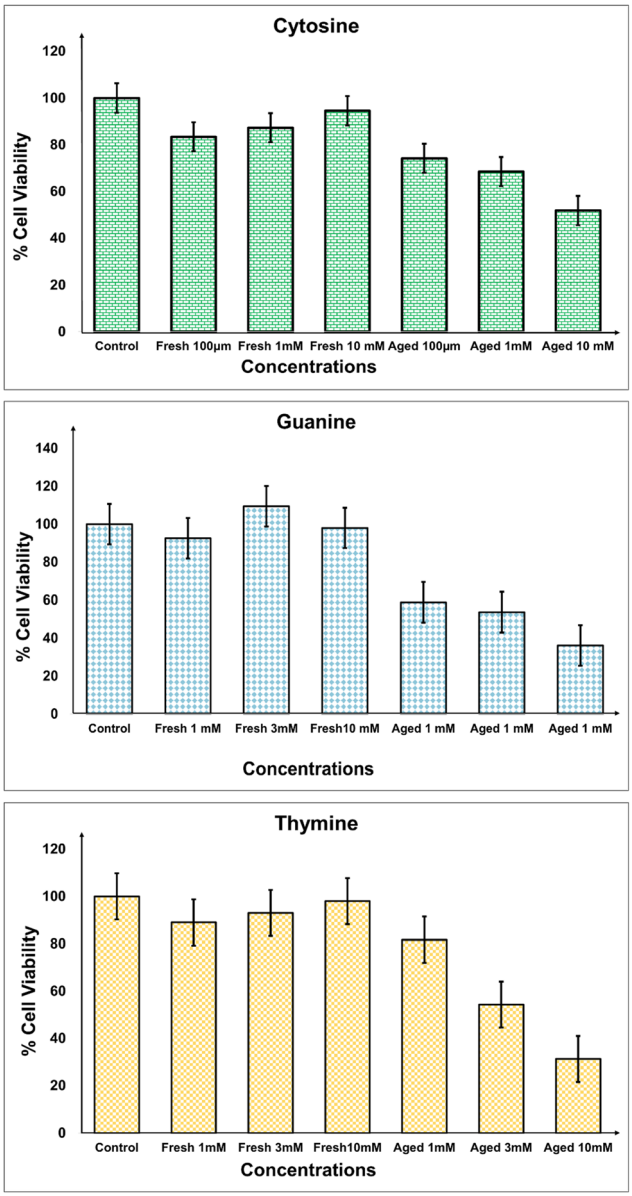

Fig. 6 Graphical representation of MTT assay in fresh and in aged conditions when co-incubated in RPE-1 cell lines with varying concentrations of cytosine, thymine and guanine.

aged nucleobases such as guanine, cytosine, and thymine. Firstly, we checked whether the introduction of these nucleobases alters the developmental process of the worms. For this, we imagined stage-wise development upon treatment with the aged samples of guanine, cytosine, and thymine. We observed that there was a developmental defect because of aged nucleobases.

Next, we performed thrashing and pharyngeal pumping assays to check for any behavioral anomalies. Thrashing assay measures the motility of worms by counting the number of to-and-fro body movements (known as "thrashes") per 10 seconds when placed in the M9 buffer, suggesting the levels of neurotransmitter dopamine.[18] We observed that there was a significant decrease in the thrashing ability of worms when subjected to the nucleobase aggregates (G, C and T) in a dose-dependent manner (Fig. 7a).

Another behavioural assay that we employed counts the rhythmic movement of contraction and relaxation of the pharynx (pharyngeal pumps).[19] It is suggestive of the feeding ability of worms. In our case, we measured the number of pharyngeal pumps per 15 seconds upon treatment with aged aggregates of nucleobases (guanine, cytosine, and thymine). We found that the pumping ability was significantly reduced upon introduction of aggregated samples in a dose-dependent manner (Figure7b).

To assess the effects of nucleobase aggregates upon physiological aspects, we checked the parameters that measure the cytotoxic activity and thermal stress resistance capability of worms. For heat shock ability we subjected the treated worms to a temperature upshift from 22 °C to 37 °C for 2.5 hours and then shifted back to 22 °C. We then counted the number of dead and live worms after 24 hours.[20] As a result, we observed that the heat shock resistance ability was reduced upon treatment with aggregates in a dose-dependent manner, meaning the maximum number of worms were dead at the highest concentration, that is 20 mM (Fig. 7c). Also, we analyzed the toxicity of these aggregates *via* MTT assay, where the colour change from yellow tetrazolium dye to insoluble purple formazan is suggestive of cell metabolic activity and viability assay.[21] In our case, we found that the viability of worms was reduced significantly with increasing concentrations of Cytosine and Thymine aggregates (Fig. 7d).

These *in vivo* results suggest that the aged samples of nucleobase aggregates (guanine, cytosine, and thymine) show toxic effects at higher concentrations and hamper the metabolism by affecting vital pathways such as body movement, stress response, and neurotransmission, reminiscent to conventional amyloidogenic proteins.[22] In future we also aim to explore the intracellular accumulation of these aggregates by designing novel *in vivo* disease models.

Mechanistic pathways linking nucleobase aggregation to disease phenotypes

The aggregation of nucleobases into amyloid-like fibrils has significant implications for disease pathophysiology, particularly in neurological and metabolic disorders. This process is reminiscent of classical protein amyloidosis, where misfolded proteins aggregate into insoluble fibrils, leading to cytotoxicity. The mechanisms underlying nucleobase aggregation-driven toxicity can be attributed to disruptions in proteostasis, membrane perturbation, and interference with cellular metabolism. The accumulation of nucleobase aggregates may interfere with protein homeostasis by sequestering molecular chaperones and degrading the efficiency of proteolytic clearance systems, which could lead to increased misfolding and aggregation of native proteins, exacerbating cellular stress. Furthermore, similar to amyloid fibrils formed by proteins, nucleobase aggregates may interact with lipid membranes, leading to structural disruption and increased permeability. This can result in ion dysregulation, oxidative stress, and

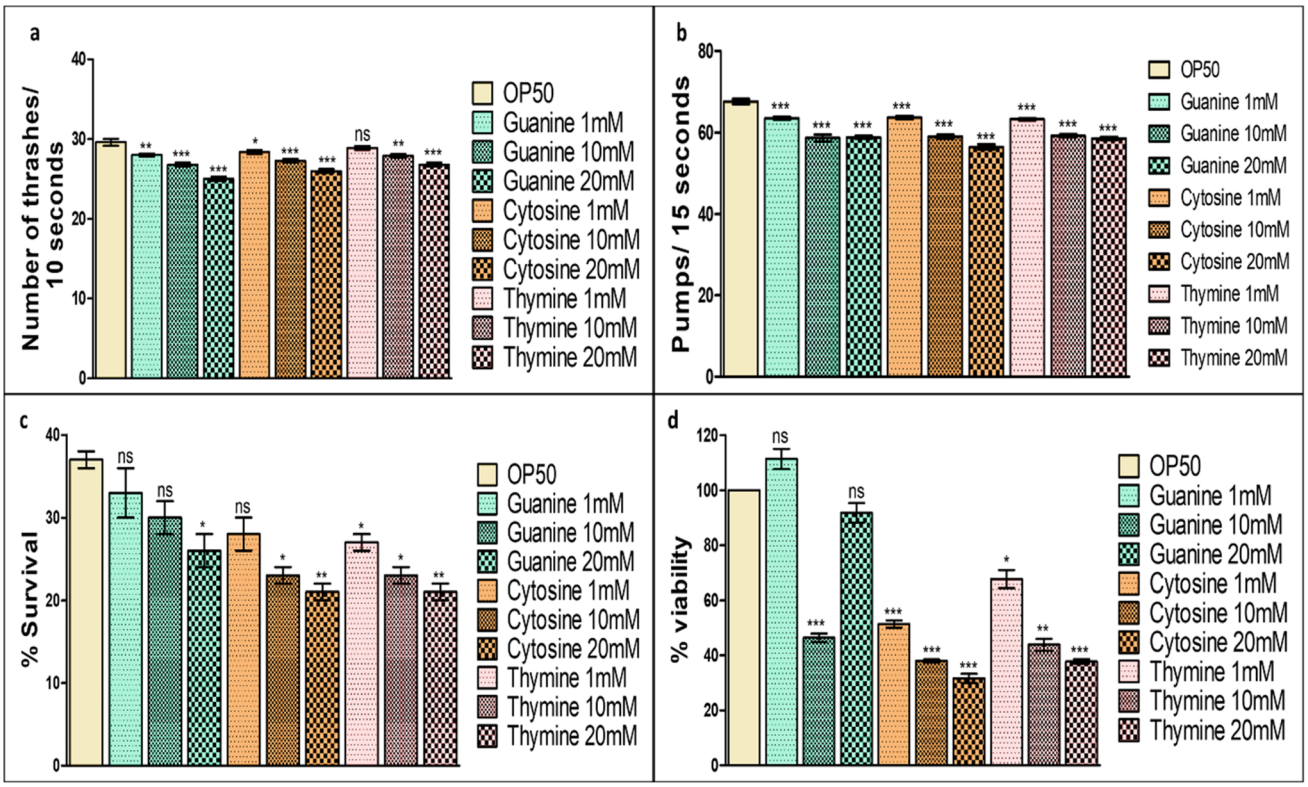

Fig. 7 (a) Thrashing assay; (b) pharyngeal pumping assay; (c) heat shock survival assay; (d) MTT assay, upon treatment with guanine (G), cytosine (C) and thymine (T) at 1 mM, 10 mM and 20 mM concentrations, employing the N2 strain of *C. elegans*.

mitochondrial dysfunction, ultimately triggering apoptotic pathways in affected cells. Inborn errors of metabolism (IEMs) such as phenylketonuria have been linked to metabolite aggregation, and the accumulation of nucleobases could impair metabolic pathways by acting as competitive inhibitors or forming toxic inclusions that alter enzymatic activity. This is particularly relevant in disorders where nucleobase metabolism is defective, potentially leading to the buildup of cytotoxic intermediates.

The results from this study further validate these mechanisms by demonstrating the cytotoxic effects of aged nucleobase aggregates in both *in vivo* and *in vitro* models. The MTT assay in RPE-1 cells indicated reduced cell viability upon exposure to these aggregates, highlighting their impact on cellular health. Moreover, the behavioral impairments observed in *C. elegans*, including reduced thrashing ability and compromised pharyngeal pumping, provide strong evidence that nucleobase aggregation disrupts fundamental biological processes, akin to neurodegenerative conditions driven by protein amyloidogenesis. These findings suggest that nucleobase aggregation is not merely a biochemical curiosity but a potential contributor to disease pathophysiology, warranting further investigation into its broader implications. Given the structural similarities between nucleobase aggregates and pathological amyloid fibrils, further exploration of their molecular interactions with cellular components, such as proteins and membranes, is essential. Future studies should aim to characterize the precise molecular pathways by which nucleobase aggregation influences disease progression, potentially revealing novel drug targets for mitigating their toxic effects.

Translational implications for clinical and therapeutic applications

Understanding the propensity of nucleobases to form amyloid-like aggregates provides crucial insights into potential clinical and therapeutic applications. These findings can be leveraged in several key areas, including disease diagnosis, therapeutic intervention, and personalized medicine. The presence of nucleobase aggregates in biological fluids or tissues could serve as novel biomarkers for the early diagnosis of metabolic disorders. The use of amyloid-specific dyes such as Thioflavin T and Congo Red, as demonstrated in this study, provides a potential diagnostic tool for detecting nucleobase aggregation in patient samples. Given the cytotoxic nature of nucleobase aggregates, the development of aggregation inhibitors could be a promising therapeutic strategy. Small molecules such as tannic acid, which was shown to disrupt nucleobase fibrillation, could be further explored as potential therapeutic agents. Additionally, chaperone-mediated approaches or proteasome activation strategies could help mitigate the cellular stress associated with nucleobase accumulation.

The implications of nucleobase aggregation extend beyond fundamental biochemistry, offering potential avenues for targeted interventions. Understanding the role of nucleobase aggregation in IEMs could aid in developing personalized

treatment strategies. Enzyme replacement therapy, targeted metabolic interventions, or gene editing techniques could be explored to reduce the levels of nucleobases prone to aggregation, thereby preventing disease progression. By integrating these insights, this research lays the foundation for future studies aimed at elucidating the pathological consequences of nucleobase aggregation and developing novel therapeutic interventions to mitigate its impact. Ultimately, recognizing nucleobase aggregation as a disease-relevant phenomenon opens new possibilities for both diagnostic and therapeutic advancements in metabolic and neurodegenerative disorders. Establishing a deeper understanding of nucleobase aggregation mechanisms and their pathological consequences will be critical in leading future therapeutic development, particularly in disorders where nucleobase metabolism is dysregulated.

Conclusion

The ability of adenine, uracil, cytosine, thymine, and guanine to self-assemble has been examined in detail using a variety of microscopy and spectroscopic techniques. Our findings indicate that aged nucleobase aggregates undergo structural transformations leading to fibrillar morphologies, which display amyloid-like properties. These properties are supported by their enhanced Thioflavin T fluorescence, Congo red birefringence, and cytotoxic effects observed in both *in vitro* and *in vivo* models. The MTT assay in RPE-1 cells demonstrated reduced cell viability upon exposure to these aggregates, while behavioral impairments in *C. elegans* suggest metabolic and physiological disruptions.

Although nucleobase aggregates share certain biophysical and cytotoxic characteristics with amyloidogenic proteins, their structural and mechanistic similarities to conventional amyloid fibrils require further investigation. Unlike protein-derived amyloids, these nucleobase assemblies may exhibit distinct modes of aggregation and toxicity, potentially influenced by their non-peptide nature and unique molecular interactions. Nonetheless, the observed fibrillar assemblies and their impact on cellular metabolism support the broader hypothesis that metabolite aggregation could contribute to disease pathophysiology. Future studies should focus on elucidating the precise molecular mechanisms underlying the nucleobase aggregation and its potential role in metabolic and neurodegenerative disorders.

Experimental section

Self-assembly studies

Sourced from JSK Fine Chemicals and Sigma Aldrich Chemical Pvt. Ltd., respectively, the materials adenine, uracil, cytosine, thymine, and guanine were used without further purification (adenine 99%, uracil 99%, cytosine 99%, thymine 99%, and guanine 98% purity). The stock solution of guanine, thymine, and cytosine was made in 1% DMSO. JSK Fine Chemicals provided experimental DMSO, methanol, and THF, while Millipore Instruments provided the deionized water. 99% pure analytical grade solvents were all that were used. At various intervals, these solutions were incubated at room temperature. For each sample, an optical microscopy analysis was performed by drop casting 20 μL of the sample onto a glass slide and letting it dry. Following sample drying, images were taken with a Leica DM2500 microscope at 40× and 63× magnification. The SEM images were taken using a Nova Nano FEG-SEM 450 microscope, which was operated at an accelerating voltage of 5 to 15 kV. The SEM samples were prepared using silicon wafers. An FEI Tecnai 20 U Twin Transmission Electron Microscope was utilised for TEM investigations, and 400 mesh carbon-coated copper grids were used to dry the materials. Using an ARC2 controller, an Asylum Research OXFORD atomic force microscope (MFP3D) was used for AFM. The analyses made use of AFM tips (AC240TS-R3) with a radius of roughly 7 nm from Asylum Research Probes. 10 μL of an aqueous nucleobase solution was drop cast, and then allowed to dry to generate AFM samples. Using a Shimadzu IR Affinity-1S spectrophotometer, the FTIR analysis of the nucleobase solution was performed at a concentration of 1 mM in D2O solvent. The nucleobases were co-incubated in a 1 : 1 ratio with urea and tannic acid for the coincubation experiment. The 99% pure TA and urea were bought from Sigma-Aldrich and Avra Chemicals. Using a Cary Eclipse Fluorescence Spectrophotometer, the ThT assay of nucleobases in solution was carried out, and the fluorescence spectra were recorded. All of the data were recorded at an excitation wavelength of 450 nm using an emission slit and an excitation wavelength of 5 nm. The 99 percent pure ThT used in the research was acquired from SRL. Our lab employed previously published techniques to prepare samples for spectroscopy and microscopy. All other results of the performed experiments are provided in the ESI.†

MTT protocol

Retinal pigmented epithelial cells (RPE1 cells) were obtained from the laboratory of Prof. Ludger Johannes, U1143 Institut Curie, Paris and were grown to confluency and then seeded into 96 well plates at a seeding density of 6000 cells per well. The nucleobases were added in two groups, aged and fresh. The aged groups had nucleobases incubated within the wells prior to the introduction of the cells, while the fresh condition incorporated the addition of nucleobases during cell seeding. The cells were then incubated for 24 hours in both of these conditions, followed by an MTT assay. Before the addition of the MTT compound, the used medium was removed, followed by PBS washing. The MTT solution was prepared at 5 mg mL^{-1} concentration and the cells were then kept for 4 Hours for incubation. At the end of the incubation, the MTT solution was removed gently, without shaking, and the same amount of DMSO was added to dissolve the formazan crystals within the wells. The plate was then covered and placed on a rocker to dissolve the crystals uniformly. The RPE1 cells, without any compound, acted as our control. The absorbance of the dissolved crystal was recorded at 562 nm, and then the graph was plotted in GraphPad Prism.

In vivo analysis of a nucleobase on the *C. elegans* model

(a)*C. elegans* cultivation and maintenance: The wild type strain *C. elegans* N2 (Bristol) was utilized in the investigations. The

strain was developed in accordance with established protocols. A nematode growth medium (NGM) was prepared by combining 50 mM sodium chloride, 2.5 g L^{-1} peptone, and 17 g L^{-1} agar with 975 mL of double-distilled water. After that, this mixture was autoclaved for 45 minutes at 15 psi pressure and 121 °C. Following that, the medium was allowed to cool to a temperature of between 50 °C and 60 °C before adding 5 g mL^{-1} ethanol-dissolved cholesterol solution, 1 mM calcium chloride, 1 mM magnesium sulphate, and 25 mM potassium dihydrogen phosphate. Standard operating procedures were followed in the propagation of *C. elegans*. Each experiment was carried out at a temperature of 22 °C in a Thermo Scientific Lab-Tech B.O.D. incubator. Synchronous worms were created following a standard protocol for embryo isolation. The worms were washed with M9 buffer, then treated with an axenizing solution (2 mL sodium hypochlorite and 5 mL of 1 M sodium hydroxide solution). The eggs were then removed from the worms' bodies and sewed onto the NGM Petri-plate that contained metabolites. The nucleobase had been aged for 10 days at 37 °C before being seeded onto NGM plates with the *Escherichia coli* (*E. coli*) OP50 strain and incubated overnight at 22 °C. (b) OP50 strain of *Escherichia coli* (*E. coli*) culture for worm feeding: 300 mg KH_2PO_4, 600 mg Na_2HPO_4, and 500 mg NaCl were combined with distilled water to create 100 mL of *E. coli* OP50 (Uracil auxotroph) culture. After that, the combination was autoclaved for 45 minutes at 15 psi pressure and 121 °C. A shaker (New Brunswick Scientific Innova42, Incubator shaker series) operating at 180 rpm was added after 500 μL of *E. coli* OP50 inoculum, 200 μL of Uracil (2 mg mL^{-1} of Milli-Q water), 1 mL of dextrose (200 mg mL^{-1} of Milli-Q water), 100 μL of $MgSO_4$, and 1 mL of NH_4Cl were added. In order to make OP50 lawns, 500 μL of *E. coli* OP50 culture was placed on NGM plates that had previously been prepared in a Bio-Safety Cabinet (Thermo Scientific 1300 series A2). The plates were then incubated at 22 °C for the whole night. (c) Imaging of worms at different developmental stages using an Olympus SZX16 microscope: We did this to check if the nucleobase therapy affected the worms' growth in any manner. In order to accomplish this, synchronised phases (embryos- > L1- > L2- > L3- > L4) on an NGM plate seeded with nucleobase were watched during their development, and images were taken at a 1× magnification. (d) Thrashing test: The worms' rate of body movement is evaluated in this test. It indicates the amount of dopamine present because it is essential for worm movement. Employing embryo isolation, 52 N2 worms were grown on OP50 seeded NGM plates and then age-synchronized onto nucleobase seeded NGM. After the worms had been incubated with the treatment for 48 hours, a drop of M9 buffer and one worm at a time were placed on a glass slide, and the number of thrashes—the movement of the body from one side to the opposite side and back to the original side—was counted. Using an Olympus SZX16 microscope at 1× magnification, the mean of the thrashes ($n = 10$) was counted for each worm after every 10 seconds. The significance was assessed using Student's *t*-test and GraphPad Prism 5 software. The experiment was repeated in duplicate for every group. (e) Pharyngeal pumping assay: This test indicates how well the worms are fed. Pharyngeal bulbs contract and relax in unison, and this number is counted. In summary, N2 worms were grown on OP50 seeded NGM plates and then, *via* embryo isolation, age-synchronized onto nucleobase seeded NGM.52. After 48 hours of treatment incubation, the worms' pharyngeal activity was examined under an 8× Olympus SZX16 microscope. Student's *t*-test and GraphPad Prism 5 software were implemented to count the average number of pharyngeal pumps ($n = 10$), and the significance was assessed. The experiment was repeated in duplicate for every group. (f) MTT test in *Caenorhabditis elegans*: This is a colorimetric test in which the biological activity of living cells reduces the 3-(4,5-dimethylthiazol-2-yl)-2,5-diphenyl tetrazolium bromide (MTT) dye to form insoluble formazan crystals of dye. This assay has also been standardised for use in *C. elegans* worms. In summary, three times with M9 and once with (1×) PBS, N2 strain age-synchronous young adults that had been fed a certain nucleobase were washed. In the 96-well micro-titer plate, 500 worms per 50 μL (1×) PBS were introduced to the wells. Each well containing worms received 50 μL of MTT dye (1× PBS) after the reagent was thoroughly dissolved at 10 mg mL^{-1} (MP Biochemicals, cat. No. 102227). The plates were centrifuged at 800 g for 10 minutes to remove the supernatant after they had been incubated for 3 hours at 20 °C. After adding 100 μL of DMSO, the plates were incubated for one hour at 20 °C. Utilising the BioTek Power Wave XS microplate reader, the absorbance at 575 nm was determined. The GraphPad Prism 5 software was used to perform the statistical analysis based on student's *t*-test. For each group, the graph represented the mean of two independent repeats. (g) Assay for heat shock survival: In conclusion, N2 worms were raised on NGM plates seeded with OP50 and age-synchronized by embryo isolation onto NGM plates seeded with a nucleobase. After 48 hours, 50 worms from each group were chosen, moved to a newly nucleobase seeded plate, and subjected to a 2.5-hour temperature change from 22 °C to 37 °C. The plates were transferred to an incubator at 22 °C after the worms experienced heat shock, and their survival was evaluated 24 hours later. Worms that were motionless or insensitive to touch were considered dead. The experiment was run twice, independently, utilising two sets of data each time. Leveraging Student's *t*-test and GraphPad Prism 5 software, the statistical analysis was performed, and the graph presented the means of the two replicates.

Data availability

Data is available from the authors upon reasonable request.

Conflicts of interest

There is no conflict of interest to declare.

Acknowledgements

Dr Nidhi Gour (NG) and RD greatly acknowledge support from SERB research grant SERB SPG/2021/000521 for funding and fellowships and Indrashil University for infrastructure support. SV is supported by the JC Bose Fellowship (SERB, India). SV and

AJ acknowledge the infrastructure facilities of IIT Kanpur. Dr Aamir Nazir (AN) and Anam Naseer (A. Naseer) extend their thanks to CSIR-CDRI for providing infrastructure and support for *C. elegans* based work. Anam Naseer (A. Naseer) also acknowledges funding by the University Grants Commission for a Senior Research Fellowship (774/(CSIR-UGC NET JUNE-2019). AS thanks DST for a PMRF fellowship, and DB thanks SERB-CRG, MoES-STARS, Gujcost-DST, GSBTM and IITGN for research grants.

References

1 A. Del Prado, D. González-Rodríguez and Y. Wu, Functional Systems Derived from Nucleobase Self-assembly, *ChemistryOpen*, 2020, **9**(4), 409–430.
2 D. Soler-Polo, J. I. Mendieta-Moreno, D. G. Trabada, J. Mendieta and J. Ortega, Proton Transfer in Guanine–Cytosine Base Pairs in B-DNA, *J. Chem. Theory Comput.*, 2019, **15**(12), 6984–6991.
3 N. Gour and E. Gazit, Metabolite assemblies: a surprising extension to the amyloid hypothesis, *Curr. Opin. Chem. Biol.*, 2021, **64**, 154–164.
4 S. Naskar and N. Gour, Realization of Amyloid-like Aggregation as a Common Cause for Pathogenesis in Diseases, *Life*, 2023, **13**(7), 1523.
5 S. Moco, S. Collino, S. Rezzi and F.-P. J. Martin, Metabolomics perspectives in pediatric research, *Pediatr. Res.*, 2013, **73**(2–4), 570–576.
6 A. Bleem and V. Daggett, Structural and functional diversity among amyloid proteins: agents of disease, building blocks of biology, and implications for molecular engineering, *Biotechnol. Bioeng.*, 2016, **114**(1), 7–20.
7 D. Laor, D. Sade, S. Shaham-Niv, D. Zaguri, M. Gartner, V. Basavalingappa, A. Raveh, E. Pichinuk, H. Engel, K. Iwasaki, T. Yamamoto, H. Noothalapati and E. Gazit, Fibril formation and therapeutic targeting of amyloid-like structures in a yeast model of adenine accumulation, *Nat. Commun.*, 2019, **10**(1), 62.
8 S. Shaham-Niv, L. Adler-Abramovich, L. Schnaider and E. Gazit, Extension of the generic amyloid hypothesis to nonproteinaceous metabolite assemblies, *Sci. Adv.*, 2015, **1**(7), e1500137.
9 B. Koshti, V. Kshtriya, R. Singh, S. Walia, D. Bhatia, K. B. Joshi and N. Gour, Unusual Aggregates Formed by the Self-Assembly of Proline, Hydroxyproline, and Lysine, *ACS Chem. Neurosci.*, 2021, **12**(17), 3237–3249.
10 B. Koshti, V. Kshtriya, C. Nardin and N. Gour, Chemical Perspective of the Mechanism of Action of Antiamyloidogenic Compounds Using a Minimalistic Peptide as a Reductionist Model, *ACS Chem. Neurosci.*, 2021, **12**(15), 2851–2864.
11 J. L. Lábár, Consistent indexing of a (set of) single crystal SAED pattern(s) with the ProcessDiffraction program, *Ultramicroscopy*, 2005, **103**(3), 237–249.
12 M. K. Siddiqi, P. Alam, S. K. Chaturvedi, M. V. Khan, S. Nusrat, S. Malik and R. H. Khan, Capreomycin inhibits the initiation of amyloid fibrillation and suppresses amyloid induced cell toxicity, *Biochim. Biophys. Acta, Proteins Proteomics*, 2018, **1866**(4), 549–557.
13 L. P. Jameson, N. W. Smith and S. V. Dzyuba, Dye-Binding Assays for Evaluation of the Effects of Small Molecule Inhibitors on Amyloid (Aβ) Self-Assembly, *ACS Chem. Neurosci.*, 2012, **3**(11), 807–819.
14 M. Biancalana and S. Koide, Molecular mechanism of Thioflavin-T binding to amyloid fibrils, *Biochim. Biophys. Acta, Proteins Proteomics*, 2010, **1804**(7), 1405–1412.
15 S. Shaham-Niv, P. Rehak, D. Zaguri, A. Levin, L. Adler-Abramovich, L. Vuković, P. Král and E. Gazit, Differential inhibition of metabolite amyloid formation by generic fibrillation-modifying polyphenols, *Commun. Chem.*, 2018, **1**(1), 25.
16 D. Sade, S. Shaham-Niv, Z. A. Arnon, O. Tavassoly and E. Gazit, Seeding of proteins into amyloid structures by metabolite assemblies may clarify certain unexplained epidemiological associations, *Open Biol.*, 2018, **8**(1), 170229.
17 S. Nandi, A. Mukhopadhyay, P. K. Nandi, N. Bera, R. Hazra, J. Chatterjee and N. Sarkar, Amyloids Formed by Nonaromatic Amino Acid Methionine and Its Cross with Phenylalanine Significantly Affects Phospholipid Vesicle Membrane: An Insight into Hypermethioninemia Disorder, *Langmuir*, 2022, **38**(27), 8252–8265.
18 E. J. Martinez-Finley, S. Chakraborty, S. Caito, S. Fretham and M. Aschner, C. elegans and Neurodegeneration In Caenorhabditis Elegans: Anatomy, Life Cycles and Biological Functions, *Adv. Med. Biol.*, 2012, **44**, 1–46.
19 D. Raizen, B. M. Song, N. Trojanowski and Y. J. You, Methods for measuring pharyngeal behaviors, *WormBook*, 2012, 1–13.
20 A. Nussenzweig, P. Burgman and G. C. Li, The role of heat-shock proteins in thermotolerance, *Philos. Trans. R. Soc., B*, 1993, **339**(1289), 279–286.
21 C. E. James and M. W. Davey, A rapid colorimetric assay for the quantitation of the viability of free-living larvae of nematodes in vitro, *Parasitol. Res.*, 2007, **101**(4), 975–980.
22 G. Guetens, G. De Boeck, M. Highley, A. T. Van Oosterom and E. A. De Bruijn, Oxidative DNA Damage: Biological Significance and Methods of Analysis, *Crit. Rev. Clin. Lab. Sci.*, 2002, **39**(4–5), 331–457.